Atomic Position Recovery by Iterative Optimization of Reconstructed Intensities: Overcoming Limitations of Holographic Crystallography

D. K. Saldin,[a] X. Chen,[a] and N. C. Kothari
Department of Physics, University of Wisconsin–Milwaukee, P.O. Box 413, Milwaukee, Wisconsin 53201

M. H. Patel
Department of Industrial and Systems Engineering, University of Wisconsin–Milwaukee, P.O. Box 784, Milwaukee, Wisconsin 53201
(Received 19 June 1992)

We propose a rapid new iterative scheme for accurately reconstructing the relative positions of source and scatterers directly from the data of a monoenergetic point-source diffraction pattern. It takes account of the squared object-wave terms neglected in traditional holographic algorithms, does not suffer from a twin-image problem, and even identifies the chemical species of the *scattering* atoms.

PACS numbers: 61.14.Dc, 42.40.–i, 79.60.–i

A by-product of the proposal [1] to reconstruct structural data from a diffraction pattern by computer holography has been the stimulation of new thought about direct methods [2] in crystallography. The earliest [3] of the holographic reconstruction algorithms used in practice was based entirely on analogy with ideas current in optics, and which stem from the seminal work of Gabor [4]. More reliable algorithms for holographic crystallography [5] have been developed subsequently which include corrections for the anisotropies of atomic scattering factors [6–9], and that of the reference wave [8,10].

A problem which was recognized early [5(c),6] was the fact that the object waves are not always much smaller in magnitude than the reference wave, giving rise to artifacts on reconstructed "images" [11,12]. Algorithms which combine data from diffraction patterns due to electrons of several different energies have been proposed [13] in part to overcome the problem of holographic twin images [3]. However, with present technology, collection of photoelectron diffraction data over a large solid angle range at several regularly spaced energies is a rather laborious task (and may be impossible with Auger electrons). We present in this Letter a robust new reconstruction algorithm, which offers the prospect of overcoming all the above difficulties, using data from a single monoenergetic diffraction pattern.

We begin by drawing attention to some of the limitations of prior schemes [3,6–10], for the reconstruction of the positions of atomic scatterers of different chemical species, from a single diffraction pattern, when the scatterers lie on both sides of an emitter atom. We illustrate our point by considering a Ni-C-O linear chain model of a CO molecule adsorbed on the atop site of a Ni surface. The interference between, say, *s*-wave electrons emitted from the C atom (forming a reference wave *R*) and those scattered from the nearby O and Ni atoms (the object waves *O*) gives rise to a far-field diffraction pattern which will have an azimuthal symmetry about a polar axis directed from the C atom towards the O. In Fig. 1 we show the polar-angle variation $I(\theta)$ of the intensity of this diffraction pattern, for 500 eV electrons, and θ lying in the range 0° to 70°, as calculated by an exact multiple-scattering cluster scheme [9].

We first use Barton's Helmholtz-Kirchhoff algorithm [3] to reconstruct the image intensities along a line passing through the three atoms in our model. The resulting radial image function (RIF) is shown in Fig. 2(a). The vertical dashed line on the positive side of the abscissa denotes the position of the O scatterer relative to the emitter (the C atom, at the origin), while that on the negative side represents the position of the Ni atom. Note the symmetry of the RIF about the origin as a consequence of the holographic twin problem. No particular indication of the O or Ni atoms is present on the RIF.

We next utilize a scattered-wave included Fourier

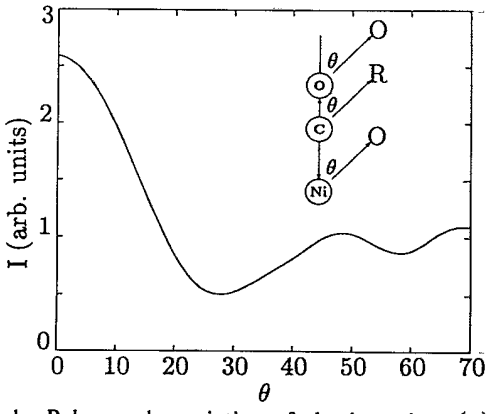

FIG. 1. Polar angle variation of the intensity $I(\theta)$ of the diffraction pattern formed by the emission of an *s*-wave electron from the C atom of the Ni-C-O linear atomic chain shown, as calculated by an exact multiple-scattering scheme. The inset shows the atomic geometry and the directions of the scattering paths. The polar axis is defined to lie in the direction from the C to the O atom. The Ni-C and C-O distances were taken to be 1.8 and 1.15 Å, respectively.

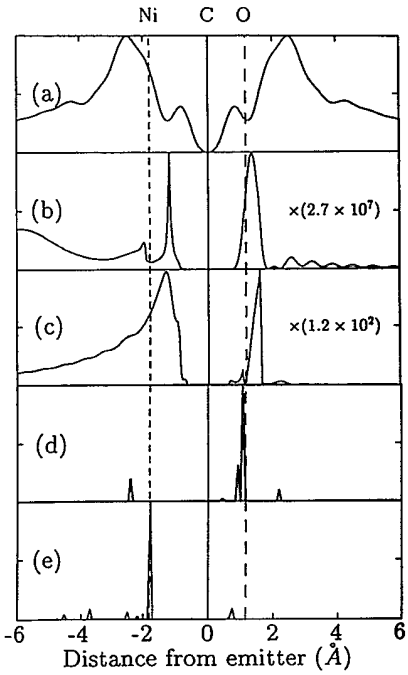

FIG. 2. Radial image functions (RIFs) along the atom chain as reconstructed from the diffraction intensities of Fig. 1 by various methods. (a) Barton's Helmholtz-Kirchhoff integral. (b) A scattered-wave-included Fourier transform (SWIFT) algorithm with a scattered-wave kernel containing a spherical-wave electron scattering factor of an O atom. The profiles on the positive side of the abscissa are multiplied by the scale factor shown to compensate for an inverse kernel containing large forward-scattering factors. (c) Same as (b) except using a scattered-wave kernel of Ni. (d) The distribution $p_O^{(4)}$ for O, as calculated by the APRIORI algorithm after four iterations. (e) The corresponding distribution $p_{Ni}^{(4)}$ for Ni, found by the same optimization process. The vertical dashed lines represent the positions of the Ni and O scatterers assumed in the calculation of $I(\theta)$ in Fig. 1.

transform (SWIFT) [7–9] to calculate the corresponding RIFs, using the spherical-wave scattering factors (4) of O and Ni separately in the scattered-wave kernel. The resulting RIFs are shown in Figs. 2(b) and 2(c), respectively. In Fig. 2(b) a peak is indeed seen close to the position of the O atom, but a quite spurious one is also seen on the opposite side of the emitter, where no O atom is present. The latter feature is either due to the incomplete removal of the twin image of the O or else due to the incomplete filtering out of the image of the Ni atom. The profile shown in Fig. 2(c) shows a peak close to the Ni atom, but also an unwanted artifact on the other side of the scatterer.

Szöke [14] has recently pointed out that many of the spurious features on holographically reconstructed images, like those in Figs. 2(a)–2(c), are a consequence of the use of back-propagation algorithms, with their attendant diffraction limits and problems of wave interference. Since the aim of holographic crystallography is the determination of the *positions* of scatterers rather than their scattered wave fields, he suggested introducing into the theory the idea of a spatial distribution function to be determined from the experimental data and a knowledge of the forms of the reference and scattered waves. We propose here a novel algorithm for determining such a function, which we term atomic position recovery by iterative optimization of reconstructed intensities (APRIORI).

Consider first the kinematic expression for the amplitude of an electron wave of detected wave vector $\mathbf{k}$, emitted at the origin of a coordinate system, and scattered by atoms of chemical species X at positions specified by the vectors $\mathbf{r}_i$:

$$A(\mathbf{k}) = R(\mathbf{k}) + \sum_{X,i} p_X(\mathbf{r}_i) O_X(\mathbf{k},\mathbf{r}_i) , \tag{1}$$

where the (real) functions $p_X(\mathbf{r}_i)$ [14] represent the spatial distribution of atoms of chemical species X. We take the emitted wave function as the reference wave R of angular momentum quantum numbers lm, i.e.,

$$R(\mathbf{k}) = Y_{lm}(\hat{\mathbf{k}}) \tag{2}$$

and

$$O_X(\mathbf{k},\mathbf{r}_i) = Y_{lm}(\hat{\mathbf{r}}_i) \frac{f_X^{(l)}(\mathbf{k},\mathbf{r}_i)}{r_i} e^{i(kr_i - \mathbf{k}\cdot\mathbf{r}_i)} \tag{3}$$

as the object waves scattered by nearby atoms. Equations (2) and (3) represent amplitudes measured on a distant spherical detector approximately centered on the emitter, so we have dropped some unimportant common factors. The atomic scattering factors in (3) take the spherical-wave form [8]

$$f_X^{(l)}(\mathbf{k},\mathbf{r}_i) = \frac{1}{ik} c_l(kr_i) \sum_{l'} (2l'+1) t_{l'}^X c_{l'}(kr_i) P_{l'}(\hat{\mathbf{k}}\cdot\hat{\mathbf{r}}_i) , \tag{4}$$

where $t_{l'}^X$ is an atomic t-matrix element of angular momentum quantum number l' for the chemical species X, $P_{l'}$ a Legendre polynomial, and $c_l(kr_i)$ the polynomial coefficient of the Hankel function $h_l^{(1)}(kr_i)$ [15]. Inelastic damping is taken into account in Eqs. (2)–(4) by allowing the wave numbers k to be complex. Using Eqs. (1)–(3) we see that the intensity, $I(\mathbf{k})$ $[=|A(\mathbf{k})|^2]$, of the diffraction pattern, regarded as a function of the wave vector $\mathbf{k}$ of the detected electron, can be written

$$I(\mathbf{k}) = |R(\mathbf{k})|^2 + \sum_{X,i} p_X(\mathbf{r}_i) \left\{ [R^*(\mathbf{k}) O_X(\mathbf{k},\mathbf{r}_i) + \text{c.c.}] + O_X^*(\mathbf{k},\mathbf{r}_i) \sum_{Z,j} p_Z(\mathbf{r}_j) O_Z(\mathbf{k},\mathbf{r}_j) \right\} , \tag{5}$$

where c.c. denotes complex conjugation, and Z is another dummy index specifying a chemical element and r_j the coor-

dinate of chemical species Z.

We take as our task the determination of the spatial distributions $p_X(\mathbf{r}_i)$ [and $p_Z(\mathbf{r}_j)$]. We describe below an iterative process for determining these quantities from experimental measurements of $I(\mathbf{k})$ and calculated values of $R(\mathbf{k})$ and $O_X(\mathbf{k},\mathbf{r}_i)$ [and $O_Z(\mathbf{k},\mathbf{r}_j)$]. If we allow the position vectors $\mathbf{r}_i$ and $\mathbf{r}_j$ to take a set of values on a uniform grid of points [14] in a space large enough to include all expected positions of the scattering atoms, we may obtain an nth-order estimate $p_X^{(n)}$ of the distributions p_X, by the following method.

We define the error $E^{(n)}(\mathbf{k})$ in our nth-order estimate of the experimentally measured intensity $I_{\text{exp}}(\mathbf{k})$ at the position on the diffraction pattern specified by the detected wave vector $\mathbf{k}$ as

$$E^{(n)}(\mathbf{k}) = |R(\mathbf{k})|^2 + \sum_{X,i} p_X^{(n)}(\mathbf{r}_i) M_X^{(n)}(\mathbf{k},\mathbf{r}_i) - \mu I_{\text{exp}}(\mathbf{k}) , \tag{6}$$

where μ a constant of proportionality to be determined, and we take

$$M_X^{(n)}(\mathbf{k},\mathbf{r}_i) = [R^*(\mathbf{k}) O_X(\mathbf{k},\mathbf{r}_i) + \text{c.c.}] + O_X^*(\mathbf{k},\mathbf{r}_i) \sum_{Z,j} p_Z^{(n-1)}(\mathbf{r}_j) O_Z(\mathbf{k},\mathbf{r}_j) , \tag{7}$$

a form suggested by the terms within the curly brackets of Eq. (5). Note that $M_X^{(n)}$ contains the distributions $p_Z^{(n-1)}(\mathbf{r}_i)$ determined by the previous iteration.

For any particular iteration $n \geq 1$, we propose finding the best fit to $I_{\text{exp}}(\mathbf{k})$ by minimizing an "objective function" [16] defined by

$$\sum_{\mathbf{k}} |E^{(n)}(\mathbf{k})| \tag{8}$$

subject to the constraints that

$$\mu \geq 0 , \tag{9}$$

$$p_X^{(n)}(\mathbf{r}_i) \geq 0 \text{ for all } X \text{ and } \mathbf{r}_i \tag{10}$$

and that

$$\sum_{\mathbf{r}_i} p_X^{(n)}(\mathbf{r}_i) = N_X \text{ for all } X , \tag{11}$$

where N_X is the number of scattering atoms of type X. The problem has now been cast in a form from which it may be solved directly by, e.g., an iterative application of the simplex algorithm [17]. By this means, we find the values of the constant μ and of the distributions $p_X^{(n)}(\mathbf{r}_i)$ which minimize the errors (8) of our fit to the data points $I_{\text{exp}}(\mathbf{k})$, using the values of the distributions $p_Z^{(n-1)}(\mathbf{r}_i)$ from the previous iteration. The iterations are halted when $p_X^{(n)}(\mathbf{r}_i) \simeq p_X^{(n-1)}(\mathbf{r}_i)$, i.e., when the distributions have converged to self-consistency.

As a test of our algorithm, we simulated an "experimental" angular distribution of intensities $I_{\text{exp}}(\mathbf{k})$ equating these to a set of values of $I(\theta)$ from Fig. 1 at 64 equally spaced polar angles θ in a measurable range from 0° to 70°, where the direction $\hat{\mathbf{k}}$ is specified by the polar and azimuthal angles θ and ϕ. The spatial grid of test positions, $\mathbf{r}_i$, of the atoms was taken to be a uniform grid of 128 points in the range ± 5 Å from the C atom along the polar axis (making a grid spacing of a little less than 0.08 Å). Since we have described a self-consistency cycle, the final distributions $p_X^{(n)}$ should be quite independent of the initial values of $p_Z^{(0)}$ used in (7) to start the process. However, in our test case, we have found that taking

$$p_Z^{(0)}(\mathbf{r}_j) = \delta_{Z,X} \delta_{\mathbf{r}_i,\mathbf{r}_j} \tag{12}$$

gave rise to the most rapid convergence. This includes the square moduli of the object waves from the same atom, but excludes the corresponding cross terms from different atoms in the initial estimates of $M_X(\mathbf{k},\mathbf{r}_i)$ in (7).

We found that the distributions $p_X^{(n)}$ converged after just four iterations of the above algorithm, after which our constant of proportionality μ also converged to within a few percent of the correct value relating our "experimental" intensities $I_{\text{exp}}(\mathbf{k})$, in the arbitrary units of Fig. 1, to the theoretical expression for $I(\mathbf{k})$ in (5). The resulting distributions $p_O^{(4)}$ and $p_{\text{Ni}}^{(4)}$ for the O and Ni scatterers, respectively, are shown in Figs. 2(d) and 2(e). The largest spikes on these histograms are at the pixels closest to the positions of the O and Ni atoms, respectively. The much smaller spikes are presumably due to the multiple scattering neglected in the reconstruction algorithm. Nevertheless, the accuracy with which the positions of the scatterers are located relative to the C emitter appear in dramatic contrast to that from panels (a)–(c) in the same figure. Also notable is the complete absence of twin images in panel (d) or (e). This has been achieved without the need for multiple-energy diffraction data [13]. Perhaps most striking is the clear identification for the first time of the different chemical species. The computer time required for the reconstruction of profiles 2(d) and 2(e) by our new algorithm was comparable with those required for Figs. 2(b) and 2(c), from the SWIFT scheme.

We also tested the effects of perturbing the diffraction intensities of Fig. 1 by random Gaussian noise. We found no perceptible shifts of the reconstructed peak positions for errors, ΔI, of $\pm\sigma$ (where σ is a standard deviation) of up to 4% of the mean intensity of the diffraction pattern. Even for ΔI of up to about 12%, we found that the Ni atom peak was reproduced at the same position, with the O atom shifted just three points of our spatial grid (i.e., about 0.2 Å). This is an encouraging indication of the stability of our technique even in the presence of fairly noisy experimental data.

In the above example, of course, the chemical species of the scatterers, and the number N_X of atoms of each species were known beforehand. In an application of our algorithm to real experimental data, the sums over X and Z above could be restricted to the chemical elements

known to constitute the sample, as determined by, e.g., an Auger or photoelectron spectrum.

It might be argued that the particular example we have presented above to illustrate our method belongs to a class of atomic geometries, which includes the case of a source atom forming part of a simple adsorbate on a surface, in which the scattering is fairly kinematical, and that our technique may not be so applicable, for example, when the sources are buried deep beneath a surface, when strong multiple-scattering effects may be unavoidable. However, we argue that it may be possible to handle the problem of structure *refinement* by an adaptation of our method even in much more general geometries. It should be noted that, in a typical problem in surface crystallography, the relative positions of most of the atoms affecting the measured intensities are assumed known, and effort is directed towards determining the positions (or small displacements from certain reference positions) of a few of them. We may then redefine our reference wave $R(\mathbf{k})$ as being not just that emitted by a single atom, but that arising after the scattering of emitted wave from some known reference structure [14], as calculated by a full multiple-scattering computer program. It is then often reasonable to regard the scattering of this reference wave from the small number, which we reidentify as N_X for species X, of atoms of unknown positions (or which deviate from their positions in the reference structure) as being kinematic, as assumed, for example, in the "tensor LEED" (low-energy electron diffraction) technique [18]. For such a problem a kinematic treatment of the object waves in a reconstruction algorithm would be no limitation.

More generally, it is possible that our method may be extended to include some multiple scattering of even the object waves. For example, if we were to include double scattering, our matrix elements $M(\mathbf{k},\mathbf{r}_i)$ would contain terms involving double and triple products of the distributions $p_Z(\mathbf{r}_j)$. A procedure can still be envisaged in which some initial guess $p_Z^{(0)}$ of these distributions is refined by the same type of iterative optimization process.

D.K.S. wishes to thank Abraham Szöke for providing his manuscript prior to publication. Acknowledgment is made to the Donors of the Petroleum Research Fund, administered by the American Chemical Society for support of this research.

---

[a]Also at the Laboratory for Surface Studies, Physics Building, P.O. Box 413, Milwaukee, WI 53211.

[1] A. Szöke, in *Short Wavelength Coherent Radiation: Generation and Applications,* Proceedings of the Topical Meeting on Short Wavelength Coherent Radiation: Generation and Applications, Monterey, California, 1986, edited by D. J. Attwood and J. Boker, AIP Conf. Proc. No. 147 (AIP, New York, 1986).

[2] M. M. Woolfson, *Direct Methods in Crystallography* (Oxford Univ. Press, Oxford, 1961).

[3] J. J. Barton, Phys. Rev. Lett. **61**, 1356 (1988).

[4] D. Gabor, Nature (London) **161**, 777 (1948).

[5] See, e.g., (a) D. K. Saldin and P. L. De Andres, Phys. Rev. Lett. **64**, 1270 (1990); (b) G. R. Harp, D. K. Saldin, and B. P. Toner, Phys. Rev. Lett. **65**, 1012 (1990); (c) S. Thevuthasan *et al.*, Phys. Rev. Lett. **67**, 469 (1991); (d) P. Hu and D. A. King, Nature (London) **353**, 831 (1991); (e) A. Stuck *et al.*, Surf. Sci. **274**, 441 (1992); (f) M. A. Mendez *et al.*, Phys. Rev. B **45**, 9402 (1992).

[6] S. Y. Tong *et al.*, Phys. Rev. Lett. **66**, 60 (1991).

[7] S. Hardcastle *et al.*, Surf. Sci. **245**, L190 (1991).

[8] B. P. Tonner *et al.*, Phys. Rev. B **43**, 14423 (1991).

[9] D. K. Saldin *et al.*, Phys. Rev. B **44**, 2480 (1991).

[10] D. K. Saldin, G. R. Harp, and B. P. Tonner, Phys. Rev. B **45**, 9629 (1992).

[11] Z.-L. Han *et al.*, Surf. Sci. **258**, 313 (1991).

[12] G. R. Harp *et al.*, J. Electron. Spectrosc. Relat. Phenom. **57**, 331 (1991).

[13] J. J. Barton and L. J. Terminello, *The Structure of Surfaces III,* edited by S. Y. Tong *et al.* (Springer, Berlin, 1991); H. Huang, H. Li, and S. Y. Tong, Phys. Rev. B **44**, 3240 (1991); S. Y. Tong, H. Li, and H. Huang, Phys. Rev. Lett. **67**, 3102 (1991); J. J. Barton, Phys. Rev. Lett. **67**, 3106 (1991).

[14] A. Szöke, Phys. Rev. B (to be published).

[15] J. J. Rehr and R. C. Albers, Phys. Rev. B **41**, 8139 (1990).

[16] See, e.g., H. A. Taha, *Operations Research: An Introduction* (Macmillan, New York, 1992).

[17] For example, W. H. Press *et al.*, *Numerical Recipes: The Art of Scientific Computing* (Cambridge Univ. Press, Cambridge, 1986).

[18] P. J. Rous *et al.*, Phys. Rev. Lett. **57**, 2951 (1986).